



HAL
open science

Feedback Classification and Optimal Control with Applications to the Controlled Lotka-Volterra Model

Bernard Bonnard, Jérémy Rouot

► **To cite this version:**

Bernard Bonnard, Jérémy Rouot. Feedback Classification and Optimal Control with Applications to the Controlled Lotka-Volterra Model. 2023. hal-03917363v1

HAL Id: hal-03917363

<https://inria.hal.science/hal-03917363v1>

Preprint submitted on 1 Jan 2023 (v1), last revised 13 Aug 2024 (v3)

HAL is a multi-disciplinary open access archive for the deposit and dissemination of scientific research documents, whether they are published or not. The documents may come from teaching and research institutions in France or abroad, or from public or private research centers.

L'archive ouverte pluridisciplinaire **HAL**, est destinée au dépôt et à la diffusion de documents scientifiques de niveau recherche, publiés ou non, émanant des établissements d'enseignement et de recherche français ou étrangers, des laboratoires publics ou privés.

2 **Feedback Classification and Optimal Control with Applications to the**
 3 **Controlled Lotka–Volterra Model**

4 Bernard Bonnard^a and Jérémy Rouot^b

5 ^aInstitut Mathématique de Bourgogne and Inria Sophia Antipolis, 9 rue Alain Savary, 21 000 Dijon

6 ^bUniv Brest, UMR CNRS 6205, Laboratoire de Mathématiques de Bretagne Atlantique, Brest

7 **ARTICLE HISTORY**

8 Compiled December 31, 2022

9 **Contents**

10	1 Introduction	2
11	2 A brief recap about singular trajectories and main result	4
12	2.1 Notations and general results	4
13	2.2 Action of the feedback group G_f on the set of good pairs	6
14	2.3 The $2d$ -case	7
15	2.4 The $3d$ -case	8
16	2.5 The general case $n \geq 3$	9
17	2.5.1 Ad-condition and the bad set of finite codimension	9
18	2.5.2 Application to generic properties of pairs (X, Y, φ)	10
19	3 Controlled Lotka–Volterra model	10
20	3.1 A brief recap about controlled Lotka–Volterra related to microbiote control	11
21	3.2 Some examples of case studies	12
22	3.2.1 The prey–predator model	12
23	3.2.2 $3d$ -case studies	13
24	3.2.3 The May–Leonard model [10]	14
25	4 Applications and numerical results	15
26	4.1 Discussion about the nonemptiness property of the good set in Theorem 2.16	15
27	4.1.1 Nonemptiness in the controlled Lotka–Volterra model	15
28	4.1.2 Emptiness in the quadratic case	15
29	4.2 The May–Leonard model	16
30	4.2.1 Geometric properties	16
31	4.2.2 Direct and semi–direct methods	17
32	4.2.3 Numerical results	18
33	5 Conclusion	19

34 **ABSTRACT**

35 Let M be a σ -compact C^∞ manifold of dimension $n \geq 2$ and consider a single–input control system: $\dot{x}(t) = X(x(t)) + u(t)Y(x(t))$, where X, Y are C^∞ vector fields on M . We prove

37 that there exist an open set of pairs (X, Y) for the C^∞ -Whitney topology such that they
 38 admit singular abnormal rays so that the spectrum of the projective singular Hamiltonian
 39 dynamics is feedback invariant. It is applied to controlled Lotka–Volterra dynamics where
 40 such rays are related to shifted equilibria of the free dynamics.

41 **KEYWORDS**

42 Feedback classification; Nonlinear systems; Lotka–Volterra model; Optimal control; Direct
 43 numerical methods

44 **1. Introduction**

45 Consider a single–input affine control system on a σ -compact C^∞ manifold of dimension
 46 $n \geq 2$ defined by

$$\frac{dx}{dt}(t) = X(x(t)) + u(t) Y(x(t)), \quad (1)$$

47 where X, Y are C^∞ vector fields on M and the set of admissible controls \mathcal{U} is the set of
 48 bounded measurable mappings $u : [0, T(u)] \mapsto \mathbb{R}$, $T(u) > 0$.

49 Let (X, Y) and (X', Y') be two such pairs. They are called *feedback equivalent* if there
 50 exist a C^∞ diffeomorphism φ on M and a feedback $u = \alpha(x) + \beta(x)u'$, where α, β are C^∞
 51 mappings and β invertible so that

52 (i) $X' = \varphi * X + (\varphi * Y) \cdot \alpha$,

53 (ii) $Y' = (\varphi * Y) \cdot \beta$,

54 where if Z is a C^∞ vector field $\varphi * Z$ is the image of Z by φ given in local coordinates by

$$\varphi * Z = \left(\frac{\partial \varphi}{\partial x} \right)^{-1} (Z \circ \varphi).$$

55 This action defines a group structure G_f on the set of triplets $\{g = (\varphi, \alpha, \beta)\}$ called the *feed-*
 56 *back group*.

57 It is well known from geometric linear system theory [17] that, restricting to linear au-
 58 tonomous controllable systems: $\dot{x}(t) = Ax(t) + u(t)b$, A being a constant matrix and b a
 59 constant vector, every such pairs (A, b) and (A', b') are feedback equivalent, restricting to
 60 linear diffeomorphisms and feedbacks: $u = \alpha \cdot x + \beta u'$, $\beta \neq 0$ constant.

61 The feedback equivalence for control affine systems was studied in the earliest reference
 62 [3] in relation with the time–minimal geodesics corresponding to the so-called *singular*
 63 *trajectories*. More precisely consider the pair (X, Y) and denote by $x(\cdot, x_0, u)$ the response
 64 to $u(\cdot) \in \mathcal{U}$ starting at time $t = 0$ from x_0 . Fixing t_f , the *fixed extremity mapping* at time
 65 t_f is the map $E^{x_0, t_f} : \mathcal{U} \ni u \mapsto x(t_f, x_0, u) \in M$. If t_f is free, the extremity mapping is the
 66 map $E^{x_0} : \mathcal{U} \ni u \mapsto x(\cdot, x_0, u)$. If we endow the set of controls with the L^∞ -norm topology
 67 both maps are Fréchet differentiable and they have singularities, that is the image of L^∞
 68 by the derivative is not of full rank n . Such a pair $(x(\cdot), u(\cdot))$ is called *singular* for the fixed
 69 time case and if the final time is not fixed such singular trajectories are called exceptional
 70 or *abnormal*.

71 Singular trajectories can be parametrized thanks to the Maximum Principle [11] as pro-
 72 jection of *singular extremal* pairs $(z(\cdot), u(\cdot))$, $z = (x, p)$ where p is non vanishing adjoint

73 vector solutions of the Hamiltonian dynamics:

$$\begin{aligned} \frac{dz}{dt}(t) &= H_X(z(t)) + u(t) H_Y(z(t)), \\ H_Y(z(t)) &= 0, \end{aligned} \quad (2)$$

74 where $H_X = p \cdot X(x)$ and $H_Y = p \cdot Y(x)$ are respectively the Hamiltonian lifts of X, Y , $H_X +$
75 uH_Y is the pseudo Hamiltonian and additionally in the abnormal case, we have:

$$H_X(z(t)) = 0.$$

76 Given a pair (X, Y) the *collinearity set* is the set \mathcal{C} of points $x \in M$ such that $X(x)$ and
77 $Y(x)$ are linearly dependent. Clearly it is a feedback invariant. Taking a point x_e in \mathcal{C} there
78 exist a *constant* u_e so that $X(x_e) + u_e Y(x_e) = 0$ and the pair (x_e, u_e) is called a forced equili-
79 brium.

80 The contribution of this article is to construct if $n \geq 2$ a set of pairs (X, Y) of codimension
81 n in the jets space such that there exist abnormal trajectories reduced to isolated point x_0 ,
82 which can be lifted into lines ℓ in the projective space $PT_{x_0}^*M$ called *abnormal rays* and
83 the whole spectrum of the *projectivized* linearized dynamics defined by (2) is feedback
84 invariant.

85 This result can be illustrated by the following $2d$ -case, $x = (x_1, x_2)$,

$$\begin{aligned} \dot{x}_1 &= \lambda x_1 + x_2^2 \\ \dot{x}_2 &= u \end{aligned} \quad (3)$$

86 in which the singular line is the axis $x_2 = 0$ on which the singular dynamics is given by
87 $\dot{x}_1 = \lambda x_1$ and the abnormal point is the equilibrium point 0. Denoting $p = (p_1, p_2)$ the
88 adjoint vector one has $p_2 = 0$ since $H_Y = 0$ and the adjoint vector is given by $\dot{p}_1 = -\lambda p_1$.
89 Hence the ray at $T_0^*\mathbb{R}^2$ is $\ell : p_1(t) = e^{-\lambda t} p_1(0)$. The singular Hamiltonian dynamics reads

$$\dot{x}_1 = \lambda x_1, \quad \dot{p}_1 = -\lambda p_1.$$

90 Clearly λ is feedback invariant and the projectivized dynamics is given by the dynamics of
91 $v = x_1/p_1$ with singular point at $v = 0$ with eigenvalue 2λ (the projectivized invariant).

92 Note that in the n -dimensional case, for each ray one gets $2n - 3$ eigenvalues to classify
93 the systems.

94 This result is applied to analyze vermin reduction for controlled *Lotka-Volterra* dyna-
95 mics in the cone $M = \mathbb{R}_{\geq 0}^n$ where the equations read

$$\frac{dx}{dt}(t) = (\text{diag}x(t)) (Ax(t) + r + u(t)\mathcal{C}) \quad (4)$$

96 with $x := (x_1, \dots, x_n)^\top$ is the vector of interacting species, $\text{diag}x$ denotes in short the diago-
97 nal matrix with diagonal coefficients x_i , $A = (a_{ij})$ is the matrix of interaction coefficients
98 and $r = (r_1, \dots, r_n)^\top$ is the individual growth vector without interaction. The constant vector
99 $\mathcal{C} = (\epsilon_1, \dots, \epsilon_n)^\top$ describes the effect of probiotic or antibiotic agents to reduce the popula-
100 tion of the infecting agent, which can be taken as the x_1 -population. The optimal control
101 problem is a *Mayer problem*: $\min_{u(\cdot)} x_1(t_f)$, which can be formulated in the dual form as:
102 $\min_{u(\cdot)} t_f, x_1(t_f) = d$, where d is a desired amount of population x_1 at final time t_f , taken

103 as a parameter. More generally we shall consider any Mayer problem: $\min_{u(\cdot)} \phi(x(t_f))$ with
104 ϕ is a smooth mapping from M to \mathbb{R} .

105 The free motion was studied by the historical contributors Lotka and Volterra, genera-
106 lizing the prey–predator model for populations dynamics [15]. The interest of the model is
107 to get easily computable equilibria using linear analysis only. In the regular case where A
108 is invertible, the *interior equilibrium* is $x_e := -A^{-1}r$ and the dynamics is related in parti-
109 cular to interaction of x_e with the trivial boundary equilibrium 0. A large amount of liter-
110 ature was devoted to analyze the dynamics in the $2d$ or $3d$ case starting from the seminal
111 complete analysis in the prey–predator model. In particular in the case of competitive sys-
112 tems, the achievement in the $3d$ –case was the explicit analysis of the limit set of the origin
113 to determine the boundary of the basin of repulsion of this point. Related references are
114 [6, 16, 13] and in particular the May–Leonard model [10] will serve as case study. An im-
115 portant very recent application of controlled Lotka–Volterra model comes from the con-
116 trol of complex microbiota, see the work by Jones et al [7] based on the Stein et al study
117 [14] to model the *C. difficile* infection of the intestinal microbiote. It contains 11 interac-
118 tion species and can admit up to 2^{11} equilibria. Hence the analysis is a huge task. More
119 modestly we shall concentrate our computation to specific $2d$ and $3d$ models to illustrate
120 our techniques. Besides the biological applications, the controlled Lotka–Volterra model
121 allows algebraic computations of the forced equilibria, which are by construction shifted
122 equilibria of the free equilibria and hence in fine one can compute in this case, the spec-
123 trum of corresponding ray abnormal solutions.

124 This article is organized in four sections. In section 2, we make a recap of properties
125 of singular trajectories and their parametrization, thanks to the Maximum Principle as an
126 Hamiltonian dynamics in the projectivized cotangent bundle. We introduce the basic con-
127 cepts of transversality theory in the jets space [9] to formulate in a neat geometric frame-
128 work the main result of this article concerning feedback invariants. In section 3, we apply
129 this theorem to classify controlled Lotka–Volterra dynamics in dimension 2 or 3. We point
130 out some applications to controlled stability and time minimal syntheses. The final sec-
131 tion 4 relates those calculations based on the Maximum Principle in the permanent case
132 to the computations of optimal solution of vermin reduction in the sampled–data control
133 frame.

134 2. A brief recap about singular trajectories and main result

135 This section is based on the results of [3] and [4], which are briefly presented to deduce
136 the classification result. It combines the techniques from transversality theory in the jets
137 space, see [9], and elementary geometric invariant theory [5].

138 2.1. Notations and general results

139 Let M be a σ –compact C^∞ (smooth) manifold of dimension $n \geq 2$. We introduce the fol-
140 lowing notations:

- 141 • TM is the tangent space of M and T_xM is the tangent space at $x \in M$.
- 142 • T^*M is the cotangent space of M and T_x^*M is the cotangent space at $x \in M$. The
143 null section of T^*M is denoted by 0 and $(T^*M)_0 = T^*M \setminus \{0\}$. We note PT^*M the
144 projectivized cotangent space i.e. $PT^*M = T^*M/\mathbb{R}^*$ and $[z]$ is the equivalence class
145 of z in PT^*M .
- 146 • For any integer N , $J^N TM$ is the space of all N –jets of vector fields i.e. Taylor expan-

147
148
149
150
151
152
153

- sions up to order N and $JTM = \cup_{N \geq 0} J^N TM$ is the jets space.
- $VF(M)$ is the vector space of all smooth vector fields on M endowed with the Whitney topology.
 - We denote by $z = (x, p)$ the canonical coordinates on (T^*M, ω) , where ω is the Darboux form induced by the Liouville form.
 - Take $(X, Y) \in VF(M)$, the Lie bracket is calculated in local coordinates with the convention:

$$[X, Y](x) := \frac{\partial X}{\partial x}(x)Y(x) - \frac{\partial Y}{\partial x}(x)X(x).$$

154
155
156

- Given any smooth function H defined on an open subset Ω of T^*M , \vec{H} denotes the Hamiltonian vector field defined by H on Ω , $\vec{H} := (\partial_p H, -\partial_x H)$. Given H_1, H_2 on M , $\{H_1, H_2\}$ denotes the Poisson bracket:

$$\{H_1, H_2\}(z) := dH_1(\vec{H}_2(z)) = \omega(H_1, H_2).$$

157
158
159
160

- If $X \in VF(M)$, H_X denotes the Hamiltonian lift: $H_X(x) := p \cdot X(x)$. Given $(X, Y) \in VF(M)$, one has $\{H_X, H_Y\} = H_{[X, Y]}$.
- Finally, to each pair (X, Y) of vector fields on M , we associate the single-input control affine system:

$$\frac{dx}{dt}(t) = X(x(t)) + u(t)Y(x(t)), \quad u(t) \in \mathbb{R}, \quad x \in M. \quad (5)$$

161
162

The study of time-minimal trajectory of (5) leads to introduce the *extremal trajectories*: $(z, u) : [0, T] \rightarrow T^*M \times \mathbb{R}$, $T > 0$, such that

163
164
165
166
167

- (1) z is absolutely continuous, u is measurable and bounded,
- (2) $z(t) \neq 0$ (0 being the null section) for all $t \in [0, T]$,
- (3) $\frac{dz}{dt}(t) = \vec{H}_X(z(t)) + u(t)\vec{H}_Y(z(t))$ for a.e. $t \in [0, T]$,
- (4) $\vec{H}_X(z(t)) + u(t)\vec{H}_Y(z(t)) = \max_{v \in \mathbb{R}} \vec{H}_X(z(t)) + v\vec{H}_Y(z(t))$ for a.e. $t \in [0, T]$ or equivalently

$$H_Y(z(t)) = 0, \quad \text{for all } t \in [0, T] \quad (6)$$

168

since $z \mapsto H_Y(z)$ is continuous.

169
170
171

Definition 2.1. A curve $(z, u) : [0, T] \rightarrow T^*M \times \mathbb{R}$ satisfying the above conditions (1)–(4) is called a singular extremal and its projection $(\Pi_M(z, u), u) = (x, u)$ is a singular trajectory. Denoting $z = (x, p)$, p is then the adjoint (non zero) vector.

172

Proposition 2.2. Let $(z, u) = (x, p, u)$ be a singular extremal on $[0, T]$. Then:

173
174

- The Fréchet derivative of the fixed time extremity mapping $E^{x(0), t_f}$ along $(x(\cdot), u(\cdot))$ is given by the linear dynamics:

$$\dot{\delta}_1 x(t) = A(t)\delta_1 x(t) + u(t)b(t) \quad (7)$$

175
176
177

- with $A = \frac{\partial X}{\partial x}(x(t)) + u(t)\frac{\partial Y}{\partial x}(x(t))$ and $b(t) = Y(x(t))$ with initial condition $\delta_1 x(0) = 0$.
- The adjoint vector $p(\cdot)$ is orthogonal to the image of the Fréchet derivative called the first order Pontryagin space vector.

178 One can easily calculate with the Maximum Principle many singular trajectories (x, u) .
 179 Indeed deriving twice with respect to t the equation (6) we get for a.e. $t \in [0, T]$:

$$\begin{aligned} H_Y(z(t)) &= \{H_Y, H_X\}(z(t)) = 0, \\ \{\{H_Y, H_X\}, H_X\}(z(t)) + u(t) \{\{H_Y, H_X\}, H_Y\}(z(t)) &= 0. \end{aligned} \quad (8)$$

180 **Definition 2.3.** A singular extremal (z, u) on $[0, T]$ is called of minimal order if $\mathcal{R} =$
 181 $\{t \in [0, T], \{\{H_X, H_Y\}, H_Y\}(z(t)) \neq 0\}$ is dense in $[0, T]$.

182 **Proposition 2.4.** Let (z, u) be a singular extremal and \mathcal{R} be a non empty set, then:

- 183 • z restricted to \mathcal{R} is smooth,
- 184 • the set $\Sigma' = \{z, H_Y(z) = \{H_Y, H_X\}(z) = 0\}$ is invariant for the singular dynamics, which
 185 is given on Σ' by:

$$\frac{dz}{dt}(t) = \vec{H}_X(z(t)) + u_s(z(t)) \vec{H}_Y(z(t)) \quad (9)$$

186 where $u_s(z)$ is the singular dynamics feedback:

$$u_s(z) = \frac{\{\{H_X, H_Y\}, H_X\}(z)}{\{\{H_Y, H_X\}, H_Y\}(z)}. \quad (10)$$

187 **Proposition 2.5.** Let (X, Y) be a pair such that the open subset Ω of all $z \in (T^*M)_0$ such that
 188 $\{z, \{\{H_X, H_Y\}, H_Y\}(z) \neq 0\}$ is not empty. Let $H_s : \Omega \rightarrow \mathbb{R}$ be the true Hamiltonian:

$$H_s := H_X + \frac{\{\{H_X, H_Y\}, H_X\}(z)}{\{\{H_Y, H_X\}, H_Y\}(z)} H_Y \quad (11)$$

189 restricted to the set $\Sigma' : \{z, H_Y(z) = \{H_Y, H_X\}(z) = 0\}$. Then there exist an open set in $VF(M) \times$
 190 $VF(M)$ such that for any couple (X, Y) in this set, Ω is open and dense and the set of all $z \in \Sigma'$
 191 is a codimension 2 symplectic manifold of Ω for the induced symplectic form: $\omega|_{\Sigma'}$.

192 **Notations 2.6.** Restricting to such pairs \mathcal{G} (called good pairs), denote:

- 193 • $\Sigma : \{z, H_Y(z) = 0\}$ the switching surface.
- 194 • \vec{H}_s the Hamiltonian dynamics restricted to $\Sigma' \subset \Sigma$ with $\Sigma' : H_Y(z) = \{H_Y, H_X\}(z) = 0$.
- 195 • Let λ_s be the mapping $\mathcal{G} \ni (X, Y) \mapsto (\vec{H}_s, \Sigma)$.

196 2.2. Action of the feedback group G_f on the set of good pairs

197 We shall briefly recall the results of [3]. First of all, borrowed from elementary geometric
 198 invariant theory [5], we have.

199 **Definition 2.7.** Let E, F be two \mathbb{R} -vector spaces and let G be a group acting linearly on E
 200 and F . An homomorphism $\mathfrak{X} : G \rightarrow \mathbb{R}^*$ is called a character. Let \mathfrak{X} be a character. A semi-
 201 invariant of weight \mathfrak{X} is a map $\lambda : E \rightarrow \mathbb{R}$ such that $\forall g \in G, \forall x \in E, \lambda(g \cdot x) = \mathfrak{X}(g)\lambda(x)$. It is
 202 called an invariant if $\mathfrak{X} = 1$. A map $\lambda : E \rightarrow F$ is a semi-covariant of weight \mathfrak{X} if $\forall g \in G, \forall x \in$
 203 $E, \lambda(g \cdot x) = \mathfrak{X}(g)g \cdot \lambda(x)$ and λ is called a covariant if $\mathfrak{X} = 1$.

204 The action of $(\varphi, \alpha, \beta) \in G_f$ can be lifted as the action of Matthieu symplectomorphisms
 205 $\vec{\varphi}$ on T^*M defined in canonical coordinates by $x = \varphi(y), p = q \frac{\partial \varphi^{-1}}{\partial y}$. The action of (φ, α, β)

206 on (\vec{H}_s, Σ) being reduced to the action of φ only. Also note that $\Sigma : H_X(z) = 0$ codes the
 207 distribution: $x \mapsto \text{span}Y(x)$.

208 **Proposition 2.8.** *Restricting to good pairs (X, Y) , λ_s is a covariant, that is the following*
 209 *diagram is commutative:*

$$\begin{array}{ccc} \mathcal{G} \ni (X, Y) & \xrightarrow{\lambda_s} & \lambda_s(X, Y) \\ G_f \downarrow & \circlearrowleft & \downarrow G_f \\ \mathcal{G} \ni (X', Y') & \xrightarrow{\lambda_s} & \lambda_s(X', Y') \end{array} .$$

210

211 **Definition 2.9.** Let (z, u) be a singular extremal on $[0, T]$ of minimal order. The singular ex-
 212 tremal is called strict if the adjoint vector is unique up to a scalar (that is unique in PT^*M)
 213 on $[0, T]$. In the strict case, a singular trajectory $(x, u) = (\Pi_M(z), u)$ on $[0, T]$ is called

- 214 (1) *Abnormal* or exceptional if for every $t \in [0, T]$, $H_X(z(t)) = 0$,
 215 (2) *Hyperbolic* if for every $t \in [0, T]$, $H_X(z(t)) \{H_Y, H_X\}, H_Y(z(t)) > 0$,
 216 (3) *Elliptic* if for every $t \in [0, T]$, $H_X(z(t)) \{H_Y, H_X\}, H_Y(z(t)) < 0$.

217 According to the high order Maximum Principle [8], the hyperbolic trajectories are can-
 218 didates to time-minimal control, while elliptic trajectories are candidates to time-maximal
 219 control, while abnormal (exceptional) can be both.

220 2.3. The $2d$ -case

221 The $2d$ -case is a specific situation but can be used to illustrate the general result avoiding
 222 technical difficulties. Without losing any generality, one can take $M = \mathbb{R}^2$ and we denote
 223 by $x = (x_1, x_2)$ the coordinates while $p = (p_1, p_2)$ denotes the non zero adjoint vector. We
 224 introduce the following determinantal sets called respectively the *singular locus* \mathcal{S} and the
 225 *collinear locus* \mathcal{C} :

$$\mathcal{S} : \{x, \det(Y, [Y, X])(x) = 0\}, \quad \mathcal{C} : \{x, \det(Y, X)(x) = 0\}.$$

226 One will assume that Y is not vanishing so that one can choose (local) coordinates with
 227 $Y = \frac{\partial}{\partial x_2}$. Moreover we assume that \mathcal{S} and \mathcal{C} are regular and intersect transversally at the
 228 point 0 . If $D := \det(Y, [[Y, X], Y])$ is not vanishing when restricted to \mathcal{S} , the singular control
 229 is given by the feedback: $u_s(x) = -\frac{D'(x)}{D(x)|_{\mathcal{S}}}$, where $D' := \det(Y, [[Y, X], X])$. Moreover using
 230 $H_Y = 0$, the adjoint vector is such that $p_2 = 0$ identically.

231 We choose coordinates preserving Y so that \mathcal{S} coincides with the x_1 -axis. In a neigh-
 232 bourhood of 0 , using the action of the feedback group, the system reads:

$$\begin{aligned} \dot{x}_1 &= \lambda x_1 - x_2^2 + o_{x_1}(x_2^2), \\ \dot{x}_2 &= u, \end{aligned} \tag{12}$$

233 where $o_{x_1}(x_2^2)$ represents a term of order ≥ 3 in the jets space of (X, Y) along the singu-
 234 lar line, identified to the x_1 -axis (the singular dynamics being feedback equivalent to the
 235 linear dynamics).

236 Assuming $\lambda \neq 0$ and restricting the dynamics to singular line identified to $x_2 = 0$,

237 straightforward computation gives us that the singular dynamics is $\dot{x}_1 = \lambda x_1$ and is foliated
 238 by the abnormal points $x_1 = 0$, the hyperbolic arc in $x_1 > 0$ and the elliptic arc in $x_1 < 0$.

239 The adjoint dynamics using $p_2 = 0$ is defined by the adjoint system $\dot{p}_1 = -\lambda p_1 + o_{x_1}(x_2)$.
 240 Hence linearized adjoint dynamics reads: $\dot{p}_1 = -\lambda p_1$.

241 In particular, the abnormal singular point $x = 0$ lifts into a ray in the projective bundle
 242 defined by $p_2 = 0$ and $p_1(t) = e^{-\lambda t} p_1(0)$. The linearized Hamiltonian dynamics takes the
 243 form

$$\dot{x}_1 = \lambda x_1, \quad \dot{p}_1 = -\lambda p_1.$$

244 Clearly λ is a feedback invariant and using the projective coordinates $v = x_1 / p_1$, leads to
 245 the dynamics $\dot{v} = 2\lambda v$ so that 2λ is a *projectivized feedback invariant*.

246 From this analysis one deduces the following.

247 **Theorem 2.10.** *In the 2d–case there exist a nonempty open set of pairs (X, Y) for the Whit-*
 248 *ney topology such that:*

- 249 (1) *Equilibria of the singular dynamics are isolated and reduced to abnormal equilibria*
 250 *x_0 defining the singular lines in M with dynamics $\dot{x} = \lambda(x_0)x$.*
- 251 (2) *Each such point defines a ray $z(t) = e^{-\lambda(x_0)t} z_0$, $z_0 \in \ell$ (ℓ being a line in $T_{x_0}^* M$).*
- 252 (3) *The singular line is foliated into the abnormal equilibrium and hyperbolic, elliptic*
 253 *arcs.*
- 254 (4) *The eigenvalue $2\lambda(x_0)$ is a projective feedback invariant.*

255 **Remark 1.** Introducing the clock one form: $\alpha = p dx$ outside the collinear set, the singular
 256 lines are the zero of $d\alpha = dp \wedge dx$.

257 2.4. The 3d–case

258 The previous planar case can be generalized to the three dimensional case, which is a very
 259 rich situation and can be treated similarly, paving the road to the general case.

260 Using (8), we introduce the determinantal mappings:

$$\begin{aligned} D &= \det(Y, [Y, X], [[Y, X], Y]), & D' &= \det(Y, [Y, X], [[Y, X], X]), \\ D'' &= \det(Y, [Y, X], X). \end{aligned} \tag{13}$$

261 Assume that D is non zero, one has the following proposition.

262 **Proposition 2.11.**

- 263 • *Singular trajectories of minimal order are solutions of the dynamics:*

$$\frac{dx}{dt}(t) = X_s(x) := X(x) + u_s(x) Y(x), \tag{14}$$

264 where the singular controls u_s is given by the feedback:

$$u_s(x) = -\frac{D'(x)}{D(x)}. \tag{15}$$

- 265 • *The sets $D'' = 0$, $DD'' > 0$ and $DD'' < 0$ are invariant for the singular dynamics and*
 266 *correspond respectively to abnormal, hyperbolic and elliptic trajectories.*

- 267 • The adjoint vector in the projective space $PT^*\mathbb{R}^3$ is uniquely defined by the relations
 268 $H_Y = \{H_Y, H_X\} = 0$.

269 Introducing the clock form $\alpha = p dx$ defined by the relations: $H_X = 1$, $H_Y = \{H_Y, H_X\} = 0$,
 270 outside the abnormal locus $D'' = 0$, the singular trajectories are the characteristics of $d\alpha$.

271 Clearly we have:

272 **Lemma 2.12.** *The feedback group G_f acts on the singular dynamics by change of coordi-*
 273 *nates only.*

274 From which we deduce:

275 **Proposition 2.13.** *The singular points of (14) are abnormal equilibria and denoting by J*
 276 *the Jacobian matrix of (14) at such points then the whole spectrum $\sigma(J)$ is feedback inva-*
 277 *riant. Each equilibrium point x_0 defines a ray solution in the projective cotangent space*
 278 *given by $z(t) = e^{-\lambda t} z(0)$, where x_0 is the canonical projection of $z(0)$, $\lambda \in \sigma(J)$.*

279 2.5. The general case $n \geq 3$

280 In this case, more technicality is necessary, but the result follows mainly from the proof of
 281 Lemma 1 in the reference [4].

282 One needs the following.

283 2.5.1. Ad-condition and the bad set of finite codimension

284 Given a pair (X, Y) of vector fields denote by $\text{ad}X$ the operator defined by: $\text{ad}^0 X(Y) = Y$,
 285 $\text{ad}X(Y) = [X, Y]$ and inductively: $\text{ad}^k X(Y) = [\text{ad}^{k-1} X \cdot Y, Y]$ for $k \geq 2$. Denote by $\text{ad}H_X$ the
 286 induced operator on the Hamiltonians: $\text{ad}H_X \cdot H_Y = \{H_X, H_Y\}$.

287 **Definition 2.14.** For N large enough we define the following subset of $J^N TM \times J^N TM$:

- 288 (1) $B'_\ell(N)$ is the subset of all couples $(j_x^N X, j_x^N Y)$ such that:
 289 $\dim \text{span}\{X(x), Y(x), [X, Y](x)\} \leq 1$.
 290 (2) \hat{B}''_ℓ is the subset of $J^N TM \times J^N TM \times \mathbb{R}$ of all triples $(j_x^N X, j_x^N Y, a)$ such that:
 291 (i) $Y(x) \neq 0$
 292 (ii) $X(x) = aY(x)$
 293 (iii) $\dim \text{span}\{\text{ad}^k G_a(Y)(x), 0 \leq k \leq n-1, [[X, Y], Y](x)\} < n$, where $G_a = X - aY$.
 294 (3) Denote by $B''_\ell(N)$ the canonical projection of $\hat{B}''_\ell(N)$ on $J^N TM \times J^N TM$. Let $B_\ell(N) =$
 295 $B'_\ell \cup B''_\ell(N)$.

296 From the proof of Lemma 1 in [4], one has:

297 **Proposition 2.15.** *Let (X, Y) be a pair in $VF(M) \times VF(M)$ such that for all $x \in M$,*
 298 $(j_x^N X, j_x^N Y) \notin B_\ell(N)$. *Then:*

- 299 (1) *Let (z, u) be a singular extremal on $[0, T]$ such that $\dim \text{span}\{X(x(t)), Y(x(t))\} \leq 1$,*
 300 *where x is the canonical projection of z . Then $x(\cdot)$ is constant and is an abnormal*
 301 *singular arc reduced to a point x_0 .*
 302 (2) *The extremal $z(\cdot)$ is of minimal order and strict and there exist a line $\ell \in T_{x_0}^* M$ so that*
 303 *$z(t) = e^{-\lambda t} z_0$, $z_0 \in \ell$ and the control u is constant a.e. Hence $z(\cdot)$ is a ray solution.*
 304 (3) *The point x_0 is a forced abnormal equilibrium contained in the collinear set and*

305 let (A, b) be the linearized dynamics (7) at (x_0, u) , then (A, b) are constant and
 306 $\text{span}\{b, Ab, \dots, A^{n-1}b\}$ is of codimension one. The line ℓ is orthogonal to this space.

307 **Theorem 2.16** (Main theorem for $n \geq 3$). *There exist an open set of pairs (X, Y) for the C^∞ -*
 308 *Whitney topology such that:*

- 309 (1) *Every singular extremal pair (z, u) on $[0, T]$ is with minimal order and strict.*
 310 (2) *Every singular trajectory reduced to a point x_0 is abnormal and x_0 is a forced abnormal*
 311 *equilibrium associated to a ray solution $z(t) = e^{-\lambda t} z(0)$, $z(0) \in \ell$, with ℓ a line in*
 312 *$PT_{x_0}^* M$.*
 313 (3) *Every abnormal equilibrium is isolated.*
 314 (4) *The pair (A, b) is not controllable and $\text{span}\{b, Ab, \dots, A^{n-1}b\} = n - 1$. The uncontrol-*
 315 *lable mode satisfies the dynamics $\dot{x} = \lambda x$.*
 316 (5) *The whole spectrum of the linearized dynamics in $PT_{x_0}^* M$ is feedback invariant.*

317 **Proof.** The proof follows from [4] and standard linear geometric control theory. More pre-
 318 cisely, from linear theory, if the pair (A, b) is controllable, the pole placement theorem [17]
 319 asserts that one can assign every spectrum using a linear gain control: $u = kx$. On the
 320 opposite, the non controllable modes cannot be modified. In the strict case, there exist a
 321 single uncontrollable mode. □

322 2.5.2. Application to generic properties of pairs (X, Y, φ) .

323 Practically one aim of biological models is to describe equilibria and their stability prop-
 324 erty. From control point of view, one can choose Y in a given class and the Mayer cost to
 325 be maximized defines a family of terminal manifolds $N(d)$ of codimension one given as
 326 the level sets: $\{x, \varphi(x) = d\}$. Take a point $x \in N$, we denote by $n(x)$ the normal vector to
 327 N at x , and accessibility properties near the terminal point can be classified in a generic
 328 context for the C^∞ -Whitney topology on the triples: (X, Y, N) using the so-called transver-
 329 sality condition. This amounts to maximize the scalar product: $n \cdot \dot{x} = n \cdot (X + uY)$ for all u
 330 in a feasible interval, which can be taken as $[-1, +1]$.

331 This leads to stratify the final target $N(d)$ into:

- 332 • The switching locus $\Sigma : \{x \in N, n(x) \cdot Y(x) = 0\}$
 333 • The singular locus $\mathcal{S} : \{x \in N, n(x) \cdot [Y, X](x) = 0\}$
 334 • The exceptional locus $\mathcal{E} : \{x \in N, n(x) \cdot X(x) = 0\}$.

335 In particular this leads, for fixed pairs (X, Y) , to consider specific critical manifolds. In
 336 our study we consider manifolds N for which: $\Sigma \cap \mathcal{S} \cap \mathcal{E} \neq \emptyset$, to analyze

- 337 • time-minimal control syntheses,
 338 • controlled stability.

339 This will be studied in the next sections using algebraic computations of equilibria on
 340 the Lotka-Volterra models.

341 3. Controlled Lotka-Volterra model

342 **3.1. A brief recap about controlled Lotka–Volterra related to microbiote control**

343 **Definition 3.1.** A controlled Lotka–Volterra dynamics is a control system of the form

$$\frac{dx}{dt}(t) = (\text{diag}x(t)) (Ax(t) + r + u(t)\mathbf{E}) \quad (16)$$

344 with $x := (x_1, \dots, x_n)^\top \in \mathbb{R}_{\geq 0}^n$, $A = (a_{ij})$, $r = (r_1, \dots, r_n)^\top$ and $\mathbf{E} = (\epsilon_1, \dots, \epsilon_n)^\top$ are constant vec-
 345 tors, $u(t)$ represents the control intensity, which can be taken in $[0, 1]$. The free dynamics
 346 is called *regular* if the matrix A is invertible. One can extend the dynamics to the whole \mathbb{R}^n
 347 and the control intensity to the whole \mathbb{R} .

348 An *interior equilibrium* is a point x in $\mathbb{R}_{> 0}^n$ such that $Ax + r = 0$ i.e. $x = A^{-1}r$. To each
 349 Lotka–Volterra dynamics one can assign in the regular case up to 2^n equilibria by consid-
 350 ering all the induced Lotka–Volterra models with extinction of at most one species x_i (i.e.
 351 $x_i = 0$). For the controlled Lotka–Volterra model, the infecting agent population is denoted
 352 x_1 , hence vermin reduction aims to minimize the x_1 -population.

353 **Lemma 3.2.** Consider the dynamics (16) and let $\Omega = (K_1, \dots, K_n)^\top$ be an interior equili-
 354 brium. Then there exist coordinates such that the dynamics (16) can be written:

$$\dot{v}_i = -(v_i + 1) \left(\sum_{j=1}^n a_{ij}^* v_j + u\mathbf{E} \right), \quad i = 1, \dots, n. \quad (17)$$

355

356 **Proof.** Let y_i be the dimensionless coordinates $y_i = x_i / K_i$, $i = 1, \dots, n$ so that the dynamics
 357 (16) with $A \leftarrow -A$ written as $\dot{x}_i = x_i \left(r_i - \sum_{j=1}^n a_{ij} x_j + u\epsilon_i \right)$, $i = 1, \dots, n$, becomes

$$\dot{y}_i = y_i \left(r_i - \sum_{j=1}^n (a_{ij} K_j) y_j + u\epsilon_i \right), \quad i = 1, \dots, n. \quad (18)$$

358 Denote $A^* = (a_{ij}^*) = (K_i a_{ij})$. By construction, the interior equilibrium is normalized to
 359 $\Omega = (1, \dots, 1)$ so that: $r_i = \sum_{j=1}^n a_{ij}^*$. Hence (18) becomes

$$\dot{y}_i = y_i \left(\sum_{j=1}^n a_{ij}^* (1 - y_j) + u\epsilon_i \right), \quad i = 1, \dots, n.$$

360 Therefore if we set $v_i = y_i - 1$ the dynamics takes the form

$$\dot{v}_i = -(v_i + 1) \left(\sum_{j=1}^n a_{ij}^* v_j - u\epsilon_i \right), \quad i = 1, \dots, n. \quad (19)$$

361 It can be written shortly as:

$$\dot{v} = -(\text{diag}(1 + v)) (A^* v - u\mathbf{E}),$$

362 where the equilibrium is normalized to 0. □

363 Therefore this triggers to consider controlled Lotka–Volterra model of the form
 364 $-(\text{diag}(v+1))(Av - u\mathcal{E})$ for which we have the following Lemma.

365 **Lemma 3.3.** Consider the controlled Lotka–Volterra model $\dot{x} = -(\text{diag}(x+1))(Ax - u\mathcal{E})$
 366 with interior equilibrium $x = 0$. Denote $X(x) = -(\text{diag}(x+1))A$, $Y(x) = (\text{diag}(x+1))\mathcal{E}$
 367 so that $-A = \frac{\partial X}{\partial x}(0)$ and $Y(0) = \mathcal{E}$. Hence $\text{span}\{\text{ad}^k X \cdot Y(0), k = 0, \dots, n-1\} =$
 368 $\text{span}\{\mathcal{E}, A\mathcal{E}, \dots, A^{n-1}\mathcal{E}\}$. Therefore $(x, u) = (0, 0)$ is an abnormal strict singular point if and
 369 only if the rank of the Kalman matrix $K = [\mathcal{E}, A\mathcal{E}, \dots, A^{n-1}\mathcal{E}]$ is strictly less than $n-1$.

370 **Corollary 3.4.** The pair (A, b) is controllable if and only if \mathcal{E} is a cyclic vector of A .

371 This leads to easily characterize every pair (A, \mathcal{E}) using a Jordan decomposition of A
 372 such that $(0, 0)$ is an (abnormal) singular trajectory.

373 **Example 3.5.** Take a matrix A with Jordan blocks with equal eigenvalues e.g. the diagonal
 374 matrix $A = \text{diag}(\lambda_1, \lambda_1, \lambda_2)$. Then for every vector \mathcal{E} the pair (A, \mathcal{E}) is not controllable.

375 3.2. Some examples of case studies

376 3.2.1. The prey–predator model

377 This historical model [15], using the (x, y) coordinates, takes the form

$$\frac{dx}{dt} = x(\lambda_1 + \mu_1 y) + u\epsilon_1 y, \quad \frac{dy}{dt} = y(\lambda_2 + \mu_2 x) + u\epsilon_2 y, \quad (20)$$

378 which covers both the elliptic and hyperbolic case.

379 The point $\Omega = (-\lambda_2/\mu_2, -\lambda_1/\mu_1) := (K_1, K_2)$ is the interior equilibrium in the quad-
 380 rant $x, y > 0$ provided that $\lambda_1\mu_1, \lambda_2\mu_2 < 0$. Introduce the dimensionless coordinates $x \leftarrow$
 381 $x/(-\lambda_2/\mu_2)$ and $y \leftarrow y(-\lambda_1/\mu_1)$ we obtain the system:

$$\dot{x} = \lambda_1 x(1 - y) + ux\epsilon_1, \quad \dot{y} = \lambda_2 y(1 - x) + ux\epsilon_2,$$

382 where the interior equilibrium is normalized to $\Omega = (1, 1)$.

383 The Jacobian matrix at Ω is

$$J = \begin{pmatrix} 0 & -\lambda_1 \\ -\lambda_2 & 0 \end{pmatrix}$$

384 and is elliptic if $\lambda_1\lambda_2 < 0$ and hyperbolic if $\lambda_1\lambda_2 > 0$.

385 The collinearity locus is $\mathcal{C} : xy[\epsilon_2\lambda_1(1 - y) - \epsilon_1\lambda_2(1 - x)] = 0$ and contains $\Omega = (1, 1)$ by
 386 construction.

387 The singular locus is $\mathcal{S} : xy[\epsilon_1^2\lambda_2x - \epsilon_2^2\lambda_1y] = 0$ and defines the interior line for $xy \neq 0$
 388 given by $y = \frac{\epsilon_1^2\lambda_2}{\epsilon_2^2\lambda_1}x$. Hence we have:

- 389 • *Elliptic case:* $\lambda_1\lambda_2 < 0$. The singular line is not contained in the cone $x, y > 0$.
- 390 • *Hyperbolic case:* $\lambda_1\lambda_2 > 0$. The singular line is contained in the cone of positive
 391 population $x, y > 0$.

392 The crucial point of the classification is to compute abnormal points, intersection of
 393 such two interior lines. At such point, the analysis of 3.2 applies.

394 A richer situation making interacting the elliptic and hyperbolic cases is to consider the
 395 model:

$$\frac{dx}{dt} = (1 - u)X(x) + uY(x), \quad u \in [0, 1],$$

396 with

$$X = \lambda_1 x(1 - y) \frac{\partial}{\partial x} + \lambda_2 y(1 - x) \frac{\partial}{\partial y}, \quad Y = x(\lambda'_1 + \mu'_1 y) \frac{\partial}{\partial x} + y(\lambda'_2 + \mu'_2 x) \frac{\partial}{\partial y},$$

397 which leads to the system: $\dot{x} = X + u(Y - X)$ connecting the elliptic case to the hyperbolic
 398 case. It is an extension of models (16). Straightforward computations lead to an interior
 399 collinearity locus, which is defined by a quadratic mapping vs. a linear map in the prey–
 400 predator model, while the interior singular locus is defined by a cubic mapping vs. a linear
 401 map. More generally automatic computations lead to analyze all the $2d$ –cases.

402 3.2.2. $3d$ –case studies

403 The $3d$ –case is a very complicated situation due to the complexity of the classification of
 404 the singular dynamics. This is not surprising in the context of dynamical systems due to
 405 the phenomenon of chaos. For Lotka–Volterra models the situation can be tamed if we
 406 consider the case of *competitive* $3d$ –models. Restricting to this case, we shall make a brief
 407 recap of this theory based on the presentation of [2] introducing the concept of carrying
 408 simplicia and the May–Leonard model [10] as a case study.

409 **Definition 3.6.** If the Lotka–Volterra dynamics takes the form: $\dot{x} = (\text{diag } x)(r - Ax)$, where
 410 $a_{ij}, r_i > 0$ for all $i, j = 1, \dots, n$ the system is called competitive.

411 **Property 3.7.** For a competitive Lotka–Volterra system, we have:

- 412 • The equilibrium $x_e = 0$ is an unstable node.
- 413 • Every positive trajectory in the $\mathbb{R}_{\geq 0}^n$ –space is bounded.

414 The interesting case, in the non trivial case, is when the dynamics admits a unique
 415 equilibrium in the cone $\mathbb{R}_{> 0}^n$. Without loss of generality, it can be taken as $\Omega = (1, \dots, 1)$
 416 using Lemma 3.2.

417 Denoting in short by $X(x)$ the vector field $(\text{diag } x)(r - Ax)$ and by φ_t be the (local) pa-
 418 rameter group $\{\exp tX\}$, one can assume that X is complete and let $\Lambda^+(x)$ denotes the
 419 ω –limit set of a point x . Recall that $p \in \Lambda^+(x)$ if there exist a sequence $t_k \rightarrow +\infty$ such that
 420 $\exp t_k X(x) \rightarrow p$ when $k \rightarrow +\infty$. One can take [12] as a reference for the properties of such
 421 set in relation with stability analysis.

422 **Definition 3.8.** Since every positive trajectory is bounded in $\mathbb{R}_{\geq 0}^n$ the basin of repulsion of
 423 the unstable node $x_e = 0$ is bounded and its boundary is called the *carrying simplex* and is
 424 denoted by Π .

425 The following result holds [6].

426 **Theorem 3.9.** In the competitive case, every positive trajectory of the dynamics in $\mathbb{R}_{\geq 0}^n \setminus \{0\}$ is
 427 asymptotic to one trajectory in Π and Π is a Lipschitz submanifold transverse to all strictly
 428 positive direction and homeomorphic to the probability simplex: $\Delta_1 : \sum_{i=1}^n x_i = 1$.

429 **Example 3.10.** In many cases, the carrying simplex can be computed and the dynamics

430 on Π describes the asymptotic behaviours of positive trajectories. The simplest example
 431 where it differs from Δ_1 is given by the $2d$ -system:

$$\dot{x} = x(1 - x - y/2), \quad \dot{y} = y(1 - 3x - y).$$

432 The only equilibria are the origin and the non interior equilibria: $(1, 0)$ and $(0, 1)$. The car-
 433 rying simplex is the graph of the function $y(x) = (1 - x)^2$ on $[0, 1]$ and is a trajectory joining
 434 the saddle $(0, 1)$ to the attracting node $(1, 0)$.

435 Clearly the computation of this set leads to solve the global stability problem, see [16].
 436 This opens the road to the concept of *controlled stability* of a chosen point in Π using the
 437 controlled Lotka–Volterra model (see Section 4.2).

438 3.2.3. The May–Leonard model [10]

439 It is a basic model where the carrying simplex coincides for some parameters of the model
 440 with the probability simplex and where the dynamics can be investigated using *bifurcation*
 441 *analysis*. We follow the presentation of [2], see also [1].

442 **Definition 3.11.** The *May–Leonard model* is the dynamics

$$\begin{aligned} \dot{x} &= x(1 - x - \alpha y - \beta z) \\ \dot{y} &= y(1 - \beta x - y - \alpha z) \\ \dot{z} &= z(1 - \alpha x - \beta y - z) \end{aligned} \tag{21}$$

443 and we denote by $A = \begin{pmatrix} 1 & \alpha & \beta \\ \beta & 1 & \alpha \\ \alpha & \beta & 1 \end{pmatrix}$ the associated (circular) matrix.

444 **Property 3.12.** For $\alpha, \beta > 0$ and $\alpha + \beta = 2$, the carrying simplex Π coincides with the proba-
 445 bility simplex $x + y + z = 1$ and eliminating in (21) the z -variable leads to the dynamics on
 446 Π :

$$\begin{aligned} \dot{x} &= \frac{\alpha - \beta}{2} x(1 - x - 2y) \\ \dot{y} &= -\frac{\alpha - \beta}{2} y(1 - 2x - y) \end{aligned} \tag{22}$$

447 with $\alpha + \beta = 2$. The system is conservative (i.e. with zero divergence) and we have a canonical
 448 Hamiltonian system associated to

$$H(x, y) = \frac{\alpha - \beta}{2} (1 - x - y)xy$$

449 so that in the open triangle $\mathcal{T} : \{(x, y) > 0, x + y < 1\}$ all the solutions are periodic.

450 More generally for arbitrary parameters α, β the eigenvalues of A can be determined,
 451 see [10] for a discussion.

452 The equilibria points are the origin, three single population of the form $(1, 0, 0)$ and three
 453 two populations solutions of the form $(1 - \alpha, 1 - \beta, 0)/(1 - \alpha\beta)$. The interior equilibrium is
 454 $\Omega = (1, 1, 1)/(1 + \alpha + \beta)$, where the linearized dynamics is determined by the eigenvalues of
 455 A .

456 Therefore the model is a good case study to apply our analysis in particular taking the
 457 control direction Y tangent to the $2d$ -plane. This allows to get a complete classification of
 458 all cases with respect to the parameters (ϵ_1, ϵ_2) and computations associated to this exam-
 459 ple are given in Section 4.2

460 4. Applications and numerical results

461 4.1. Discussion about the nonemptiness property of the good set in Theorem 2.16

462 4.1.1. Nonemptiness in the controlled Lotka–Volterra model

463 Using example 3.5 from Section 3.1, consider the controlled Lotka–Volterra model:
 464 $-\text{diag}(x+1) [Ax - u\mathcal{C}]$ in \mathbb{R}^3 with:

- 465 • $A = \text{diag}(\lambda_1, \lambda_2, \lambda_3)$,
- 466 • $\mathcal{C} = (\epsilon_1, \epsilon_2, \epsilon_3)^\top$, $\epsilon_1 \neq \epsilon_2$.

467 Hence since the matrix A contains two identical eigenvalues, one deduces that for every
 468 \mathcal{C} , the equilibrium point $x_e = 0$ is abnormal with $u_e = 0$ being the abnormal control.

469 Symbolic computations allow to determine the determinantal mapping D, D' defined in
 470 Section 2.4 and the singular control being $u_s(x) = -D'(x)/D(x)$. By construction at $x = 0$,
 471 one has $u_s(0) = u_e = 0$.

472 But symbolic calculation yields the following spectrum of the linearized singular dyna-
 473 mics at 0 :

$$(\lambda_3 - \lambda_1, -\lambda_3, -\lambda_1).$$

474 Hence the singular point 0 is isolated, proving that the set introduced in Theorem 2.16
 475 is nonempty.

476 The calculation can be generalized to the n -dimensional Lotka–Volterra case.

477 4.1.2. Emptiness in the quadratic case

478 **Proposition 4.1.** *Let (Q, b) be a pair of vector fields on \mathbb{R}^3 with Q being a quadratic homo-
 479 geneous and b being a constant vector. Then we have:*

- 480 (1) • $D = \det(b, [b, Q], [[b, Q], b])$: linear form
 481 • $D' = \det(b, [b, Q], [[b, Q], Q])$: cubic form
 482 • $D'' = \det(b, [b, Q], Q)$: cubic form.

483 Hence the singular dynamics

$$\frac{dx}{dt}(t) = Q(x(t)) - \frac{D'(x(t))}{D(x(t))} b$$

484 is homogeneous and quadratic.

485 (2) Let be the time reparameterization defined by $Dd\tau = dt$ so that the singular dynamics
 486 reads

$$\frac{dx}{d\tau}(\tau) = Q(x(\tau))D(x(\tau)) - D'(x(\tau)) b$$

487 and is cubic. It can be projected on the projectivized space $P(\mathbb{R}^3)$. Moreover the map

$$\hat{\lambda}_s : (Q, b) \mapsto QD - D'b$$

488 is a semi-covariant.

489 **Definition 4.2.** Let $\dot{x} = H(x)$ be a differential equation on \mathbb{R}^n with H being a cubic ho-
 490 mogeneous vector field. A ray is a line ℓ so that the dynamics restricted to ℓ is given by
 491 $\dot{x}_1 = \lambda x_1^3$. In the generic case, $\lambda \neq 0$, it is an asymptotic direction but if $\lambda = 0$ it is a set of
 492 non isolated equilibria for the dynamics.

493 From which we deduce.

494 **Corollary 4.3.** For every pair (Q, b) on \mathbb{R}^3 , every abnormal equilibrium point is not isolated
 495 so that in this family the set described in Theorem 2.16 is empty.

496 Nevertheless, one can use for pair (Q, b) the projectivized singular dynamics on $P(\mathbb{R}^3)$ to
 497 compute feedback invariants. Indeed every ray projects onto an equilibrium point, where
 498 we can compute the linearized dynamics. We refer to [3] for the application of this result to
 499 classify the controlled Euler dynamics in the attitude control problem, where b describes
 500 the position of gas jet on the satellite.

501 4.2. The May–Leonard model

502 4.2.1. Geometric properties

503 Following Section 3.2.3, we take the May–Leonard model, where the free dynamics is the
 504 restriction of (21) to the carrying simplex $\Pi : x + y + z = 1$ and the control directions are in
 505 the carrying simplex i.e. we consider the system

$$\dot{\mathbf{x}} = X(\mathbf{x}) + u Y(\mathbf{x}), \quad \mathbf{x} = (x, y), \quad u \in [0, 1]$$

506 with

$$X = x(1 - x - 2y) \frac{\partial}{\partial x} - y(1 - 2x - y) \frac{\partial}{\partial y}, \quad Y = \epsilon_1 x \frac{\partial}{\partial x} + \epsilon_2 y \frac{\partial}{\partial y}. \quad (23)$$

507 The singular set and the collinearity locus are given respectively by

$$\mathcal{S} : \epsilon_2(\epsilon_1 + 2\epsilon_2)y + \epsilon_1(\epsilon_2 + 2\epsilon_1)x = 0 \quad \text{and} \quad \mathcal{C} : (\epsilon_1 + 2\epsilon_2)y + (\epsilon_2 + 2\epsilon_1)x = \epsilon_1 + \epsilon_2.$$

508 For $\epsilon_1 \neq \epsilon_2$, $\epsilon_1 \neq -2\epsilon_2$ and $\epsilon_2 \neq -2\epsilon_1$, their intersection $\mathcal{S} \cap \mathcal{C}$ is the point

$$x_{se} = \left(\frac{\epsilon_2}{\epsilon_2 + 2\epsilon_1} \frac{\epsilon_1 + \epsilon_2}{\epsilon_2 - \epsilon_1}, \frac{\epsilon_1}{\epsilon_1 + 2\epsilon_2} \frac{\epsilon_1 + \epsilon_2}{\epsilon_1 - \epsilon_2} \right) = \left(\frac{1}{1 + 2\kappa} \frac{1 + \kappa}{1 - \kappa}, \frac{\kappa}{\kappa + 2} \frac{\kappa + 1}{\kappa - 1} \right), \quad \kappa = \frac{\epsilon_1}{\epsilon_2}$$

509 and the study of the components of x_{se} as functions of κ shows that x_{se} is in the positive
 510 orthant if $\kappa \in]-\infty, -2[\cup]-1/2, 0[$ and is outside the triangle $\mathcal{T} = \{\mathbf{x} = (x, y) > 0, x + y < 1\}$ for
 511 any value of κ (recall that in the triangle \mathcal{T} the free dynamics consists in periodic orbits).

512 For $x_e = (x_{1e}, x_{2e}) \in \mathcal{C}$, the value of the control $u_e(x_e)$ such that $X(x_e) + u_e Y(x_e) = 0$ is

$$u_e(x_e) = \frac{1 - 3x_{1e}}{\epsilon_1 + 2\epsilon_2}$$

and the spectrum of the Jacobian matrix $J(x_e) := \frac{\partial}{\partial \mathbf{x}} (X(\mathbf{x}) + u Y(\mathbf{x}))|_{\mathbf{x}=x_e}$ is

$$\sigma(J(x_e)) = \left\{ 3u(\epsilon_1 + \epsilon_2) \pm \frac{1}{2\sqrt{3}} \sqrt{11u^2(\epsilon_1 + \epsilon_2)^2 + 4(\epsilon_1 u + 1)(\epsilon_2 u - 1)} \right\}.$$

513 In particular,

- 514 • at $u = 0$, $\sigma(J(x_e)) = \left\{ \pm \frac{i}{\sqrt{3}} \right\}$,
- 515 • at $u = 1$, $\sigma(J(x_e)) = \left\{ 3(\epsilon_1 + \epsilon_2) \pm \frac{1}{2\sqrt{3}} \sqrt{11(\epsilon_1 + \epsilon_2)^2 + 4(\epsilon_1 + 1)(\epsilon_2 - 1)} \right\}$,
- 516 • at $u = u_e(x_{se})$, $\sigma(J(x_e)) = \left\{ \frac{\epsilon_1 + \epsilon_2}{\epsilon_1 - \epsilon_2}, -\frac{\epsilon_1 + \epsilon_2}{\epsilon_1 - \epsilon_2} \frac{3\epsilon_1 \epsilon_2}{(2\epsilon_1 + \epsilon_2)(2\epsilon_2 + \epsilon_1)} \right\}$. Note that in this case, the first
517 eigenvalue corresponds to the noncontrollable mode of the system, while the second
518 eigenvalue is not meaningful since it can be replaced by any value via pole shifting.

519 The singular dynamics $\dot{z} = \tilde{H}_s(z)$ (restricted to Σ) has eigenvalues at $x = x_{se}$:

$$\left\{ -\frac{\epsilon_1 + \epsilon_2}{\epsilon_1 - \epsilon_2}, \frac{\epsilon_1 + \epsilon_2}{\epsilon_1 - \epsilon_2} \right\}$$

520 and $\lambda = \frac{\epsilon_1 + \epsilon_2}{\epsilon_1 - \epsilon_2}$ is a feedback invariant of the control system.

521 4.2.2. Direct and semi-direct methods

522 We present two numerical schemes to solve the time-minimal control problem for the
523 Lotka–Volterra class of models specifically a direct method and a semi-direct method.

524 The objective is to reach, from an initial position x_0 a terminal manifold of codimen-
525 sion one in minimum time, namely, this target is taken as a disk $N(\mathbf{x}) \leq 0$ centered on the
526 collinearity locus \mathcal{C} in which local controllability is guaranteed provided that the forcing
527 feedback is interior. This is an example of controlled stability.

528 There is no use comparing these methods in terms of computational time. The direct
529 method computes open-loop controls, while the semi-direct method computes closed-
530 loop controls, which can be used for real-time application since the trajectory is computed
531 step by step. In this sense we use the direct method to have an upper bound of the value
532 function and it is compared to the objective value associated to the semi-direct method
533 presented below.

534 Both methods are implemented in MATHEMATICA programming language using the
535 optimization solver FindMinimum.

536 **Direct method.** We consider the time-optimal control problem:

$$(OCP) \quad \min_{u(\cdot), T} \quad T$$

$$\begin{aligned} \dot{\mathbf{x}}(t) &= X(\mathbf{x}(t)) + u(t) Y(\mathbf{x}(t)), \quad u(t) \in [0, 1], \quad a.e. \ t \in [0, T] \\ \mathbf{x}(0) &= x_0 \text{ (given)} \\ N(\mathbf{x}(T)) &\leq 0 \end{aligned} ,$$

537 where $\mathbf{x} = (x, y)$ and X, Y are given by (23).

538 We perform a discretization over the state and the control spaces for (OCP) to obtain
 539 a nonlinear finite dimensional optimization problem. The optimization variables are the
 540 values of the control at each time step and a primal–dual interior point method is used
 541 to solve numerically the optimization problem. The optimality conditions – written as a
 542 relaxation of the Karush–Kuhn–Tucker conditions – are determined using automatic dif-
 543 ferentiation.

544 It is usually a quite robust method with respect to the initialization compared to indi-
 545 rect methods based on the Pontryagin Maximum Principle. However it does not exploit the
 546 geometric structure of the optimal control. The BOCOP software¹ provides an implemen-
 547 tation of this method based on the IPOPT optimization solver².

548 **Model predictive control method.** The semi–direct method is based on a sampled–data
 549 control formulation of the problem, which is adapted to medical protocols that can be
 550 used to cure the C. difficile infection. The optimal path is constructed iteratively, where at
 551 each iteration we solve an optimal control problem on a reduced time horizon, whereas
 552 the direct method discretizes the problem on the whole time interval.

553 In this sense, our method is closely related to model predictive control (MPC) widely
 554 used for control theory applications. The current state of the method x_c is initialized to x_0
 555 and is updated iteratively by solving the optimal control problems of the form

$$(OCP') \quad \min_{u \in \mathbb{R}^h} \quad N(\mathbf{x}(t_h; u, x_c)) \\ \dot{\mathbf{x}}(t) = X(\mathbf{x}(t)) + u_i Y(\mathbf{x}(t)), \quad u_i \in [0, 1], \quad a.e. \quad t \in [t_i, t_{i+1}], \quad i = 0, \dots, h-1, \\ \mathbf{x}(0) = x_c$$

556 where the integer h is the horizon, $0 = t_0 < \dots < t_h$ are given fixed times and $\mathbf{x}(\cdot; u, x_c)$
 557 is the state response associated to (u_1, \dots, u_h) and starting at x_c at $t = 0$. The algorithm
 558 terminates when $|N(x_c)|$ is smaller than a given threshold.

559 To solve (OCP') numerically, we derive a finite dimensional optimization problem by
 560 constructing an approximation of the objective function $u = (u_0, \dots, u_{h-1}) \mapsto N(\mathbf{x}(t_h))$ via
 561 an approximation of $\mathbf{x}(t_h; u, x_c)$ by discretizing the differential constraint with a midpoint
 562 rule (the discretization of the state on $[0, t_h]$ is finer than the partition $0 < t_1 < \dots < t_h$). The
 563 approximation of $N(\mathbf{x}(t_h; u, x_c))$ – together with its derivatives with respect to u_i , $i = 1, \dots, h$
 564 – can be computed offline using symbolic computations. Then we solve the optimization
 565 problem associated to (OCP') using a primal–dual interior point method. Once (OCP')
 566 is solved for the current value of x_c , we retrieve the values of t_1 and u_1 to update $x_c \leftarrow$
 567 $\mathbf{x}(t_1; u_1, x_c)$ and we iterate considering the resulting new instance of (OCP').

568 4.2.3. Numerical results

569 We apply the previous numerical methods to the specific May–Leonard model and our aim
 570 is to control the system in the carrying simplex Π .

571 From the computations in Section 4.2.1, we can choose ϵ_1, ϵ_2 to fix the positions of x_{se}
 572 and x_e (corresponding to $u_e = 1$) and so that the singular dynamics goes toward \mathcal{C} and
 573 is hyperbolic. The target is taken as the circle N centered on \mathcal{C} and is reachable with an
 574 admissible control $u \in]0, 1[$.

575 We fix the initial point to $x_0 = (0.1, 0.8)$. The direct method converges in about 200 ite-
 576 rations to a bang–bang–singular–bang control (see Fig. 1) and the corresponding trajectory
 577 reaches N in less than 7.7 unit of time.

¹www.bocop.org

²www.coin-or.github.io/Ipopt

578 The semi-direct method is tuned with an horizon of $t_h = 2$ unit of time with $h = 3$ i.e. we
579 compute three controls u_1, u_2, u_3 over this horizon. The resulting control seems to have the
580 same structure as the control of the direct method. The trajectory reaches N in about 12
581 unit of time (see Fig. 1). The depicted singular behavior depends on the size of the horizon
582 t_h and the number of controls on that horizon. A smaller horizon t_h would typically keep
583 the trajectory away from the singular arc.

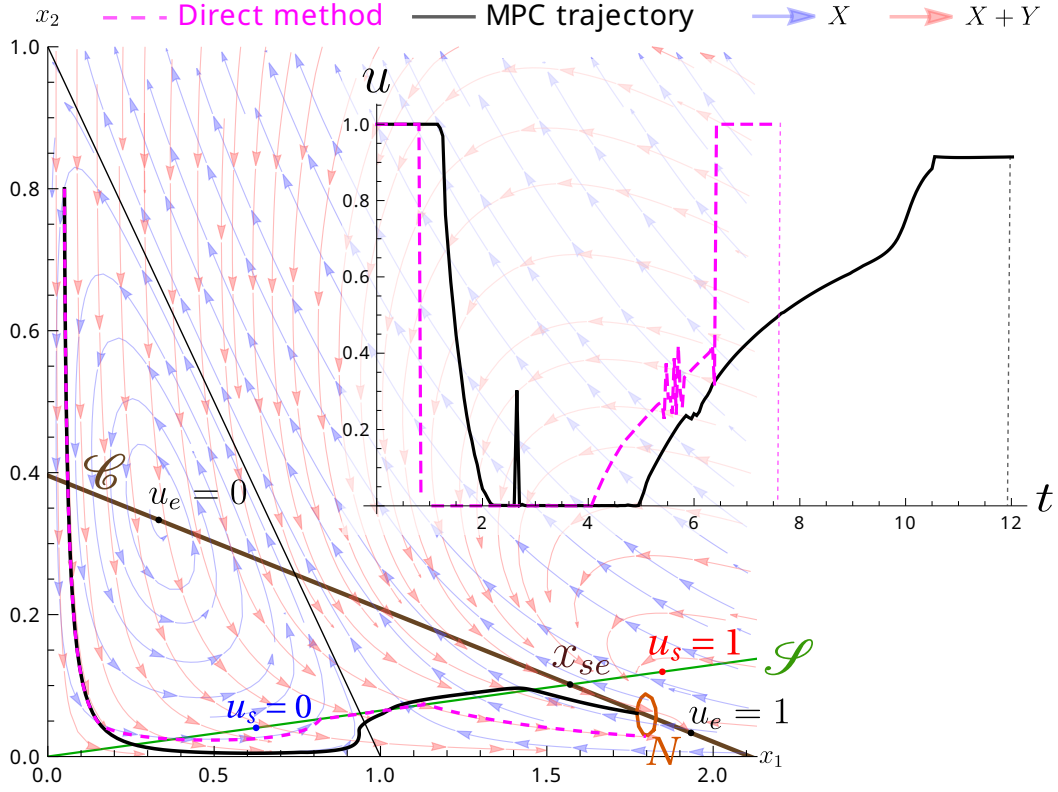


Figure 1. Geometric picture corresponding to the May-Leonard model presented in Section 4.2.3. (left) The dashed trajectory starting from $x_0 = (0.1, 0.8)$ and obtained with a direct method is bang-bang-singular-bang. It reaches the terminal circle N in less than 7.7 unit of time. The continuous MPC trajectory, obtained with an horizon of $t_h = 2$ and with three controls ($h = 3$), seems to reproduce the singular behavior. It reaches N in about 12 unit of time. (right) Time evolution of the control for the direct and MPC methods.

584 5. Conclusion

585 In this article we describe feedback invariants to classify single-input control affine systems
586 in relation with the time-minimal control problem. They can be explicitly calculated
587 using algebraic computations in the jets spaces of the dynamics at a given point corre-
588 sponding to an abnormal stationary geodesic. They correspond at such points to the spec-
589 trum of the projectivized Hamiltonian geodesic dynamics.

590 This result completes the computation of the feedback invariants related to the concept
591 of conjugate points for both normal and abnormal geodesics. This gives a neat common
592 geometric frame since those are related to the spectrum of the "projectivized" second-
593 order intrinsic derivative, in relation with algebraic computations in the jets space of
594 geodesics.

595 Our result is briefly applied to the controlled Lotka–Volterra, where abnormal stationary
596 geodesics are shifted equilibria of the free dynamics, which can be determined using lin-
597 ear calculations only. This gives an algebraic frame in relation with population dynamics
598 control. Another applications are for quadratic systems in relation for instance with the
599 attitude control problem of a rigid spacecraft.

600 A final numerical application shows the relation of the study to the time–minimal con-
601 trol problem, combining Pontryagin Maximum Principle with direct and semi–direct nu-
602 merical frame. Additionally it provides an example of controlled stability method popular
603 in biological models. More generally our analysis leads to structurally stable results based
604 on Lie algebraic computations in the jets space of the geodesics dynamics. It opens the
605 road to fine applications translating for instance results for the free dynamics of the May–
606 Leonard model [1] to controlled stability or time optimal results, in the controlled case.

607 Funding

608 This work benefited from the support of the program PEPS "Jeunes chercheurs et jeunes
609 chercheuses" of Insmi 2022.

610 References

- 611 [1] S. BAIGENT, *Geometry of carrying simplices of 3-species competitive Lotka–Volterra*
612 *systems*. Nonlinearity, **26**, no.4 (2013), pp.1001–1029.
- 613 [2] S. BAIGENT, *Lotka–Volterra Dynamical Systems*. In: S. Bullett, T. Fearn, F. Smith, eds.
614 *Dynamical and Complex Systems*, LTCC Advanced Mathematics Series: Chapter **5**.
615 Singapore: World Scientific, 2017, 227 pages.
- 616 [3] B. BONNARD, *Feedback equivalence for nonlinear systems and the time optimal control*
617 *problem*. SIAM J. on Control and Optim., **29** (1991), pp. 1300–1321.
- 618 [4] B. BONNARD, I. KUPKA, *Generic properties of singular trajectories*. Ann. Inst. H.
619 Poincaré Anal. Non Linéaire, **14**, no.2 (1997), pp. 167–186.
- 620 [5] J.A. DIEUDONNÉ, J.B. CARRELL, *Invariant Theory, Old and New*. Academic Press, New
621 York, 1971, 85 pages.
- 622 [6] M.W. HIRSCH, *Systems of differential equations which are competitive or cooperative:*
623 *III. Competing species*. Nonlinearity, **1**, (1988), pp.51–71.
- 624 [7] E.W. JONES, P.S. CLARCKE, J.M. CARSLON, *Navigation of outcome in a generalized*
625 *Lotka–Volterra model of the microbiome*. Advances in Nonlinear Biological Systems,
626 *Modeling and Optimal Control*, AIMS on applied Maths **11** (2021), pp. 97–117.
- 627 [8] A.J. KRENER, *The high order maximal principle and its application to singular ex-*
628 *tremals*. SIAM J. Control Optim. **15** no. 2, (1977) pp. 256–293.
- 629 [9] J. MARTINET, *Singularities of smooth functions and maps*. London Mathematical
630 Society Lecture Note Series, **58**. Cambridge University Press, Cambridge–New York,
631 1982, 256 pages.
- 632 [10] R.M. MAY, W.J. LEONARD, *Nonlinear aspects of competition between three species*.
633 SIAM J. Appl. Math., **29** (1975), pp. 243–253.
- 634 [11] L.S. PONTRYAGIN, V.G. BOLTYANSKII, R.V. GAMKRELIDZE, E.F. MISHCHENKO, *The math-*
635 *ematical theory of optimal processes*. Oxford, Pergamon Press, 1964, 362 pages.
- 636 [12] N. ROUCHE, J. MAWHIN, *Equations Différentielles Ordinaires*. Masson, Paris, **2** (1973),
637 266 pages.

- 638 [13] S. SMALE, *On the differential equations of species in competition*. Journal of Mathe-
639 matical Biology, **3** (1976), pp. 5–7.
- 640 [14] R.R. STEIN, V. BUCCI, N.C. TOUSSAINT, C.G. BUFFIE, G. RÄTSCH, E.G. PAMER, et al.,
641 *Ecological modelling from time-series inference: insight into dynamics and stability of*
642 *intestinal microbiota*. PLoS Comp. Biology, **9** no. 12 (2013).
- 643 [15] V. VOLTERRA, *Leçons sur la théorie mathématique de la lutte pour la vie*. Les Grands
644 Classiques Gauthier-Villars. Éditions Jacques Gabay, Sceaux, 1990, 215 pages.
- 645 [16] E.C. ZEEMAN, M.L. ZEEMAN, *From local to global behavior in competitive Lotka-*
646 *Volterra systems*. Trans. Amer. Math. Soc., 355 (2003), pp. 713–734.
- 647 [17] W.M. WONHAM, *Linear Multivariable Control*. Springer-Verlag, New York, 1985, 348
648 pages.